Undergraduate Research Journal at UCCS
Volume 2.2, July 2009

A Critical Analysis of Solid Rocket Motor Thrust Augmentation Using Beamed Power

Sean Hammerland and Barry Cornella
Dept. of Mechanical and Aerospace Engineering, University of Colorado at Colorado Springs

Abstract

With the efficiencies of current launch systems reaching their chemical limit, there is a need to investigate improved methods of placing payloads into orbit. Although being able to improve the efficiency of a vehicle by several percent is beneficial, this may only increase the overall payload mass fraction by a small amount. Beamed energy propulsion is a revolutionary technique being explored to achieve increased performance. Beamed energy propulsion is a technique which utilizes electromagnetic radiation from a remote source to increase the energy of a propellant. A possible benefit of this technique is its potential to propel a spacecraft into orbit without the addition of mass to the launch vehicle. The focus of this critical analysis was to evaluate a microwave based beamed energy propulsion system that directly couples its energy to the alumina particles exiting the nozzle of a solid rocket motor. Thrust augmentation occurs through a process of the liquid alumina droplets in the exhaust nozzle absorbing microwave energy and remaining at an elevated temperature. The absorbed microwave energy is deposited into the expanding gas through molecular collisions with the liquid alumina droplets. This analysis includes a study of the coupling coefficient of microwaves to alumina particles, an overview of the ground based microwave generation system, and launch vehicle trajectory simulations to extract performance data.

Nomenclature

A_r	=	receiver aperture area [m^2]
A_t	=	transmitter aperture area [m^2]
D	=	antenna diameter [m]
$E_{t,50km}$	=	kinetic and potential energy of the system [J]
E_{total}	=	kinetic and potential energy of the system [J]
G_{dbi}	=	antenna gain [dBi]
G_t	=	receiver gain [dBi]
G_t	=	transmitter gain [dBi]
L_{atm}	=	atmospheric transmission loss [dB]
L_{fs}	=	free space transmission loss [dB]
L_{other}	=	miscellaneous transmission losses [dB]
$\dot{m}$	=	mass flow rate of the propellant (constant) [kg]
p	=	atmospheric pressure [torr]
$P_{in\ Jet}$	=	total jet kinetic power [GW]

P_{out}	=	output power of the vehicle [GW]
P_r	=	received power [dB]
P_t	=	transmitted power [dB]
R	=	transmission range [m]
R_{ff}	=	far-field region range [m]
t_{50km}	=	total time of accent of vehicle to 50 km [s]
V_e	=	exit velocity of the propellant [m/s]
ΔV	=	velocity of the vehicle [km]

Introduction

BEAMED energy propulsion is a technique which utilizes electromagnetic radiation from a remote source to increase the energy of a propellant. The electromagnetic radiation, in general, can originate from any source, although the most recent concepts feature either high power laser beams or microwaves. One significant advantage of beamed energy propulsion is that it requires no additional mass to be carried on-board the vehicle. Beamed energy propulsion can also overcome the inherent limitations on specific impulse due to the chemical energy production mechanisms.

The idea of beamed energy propulsion was first put forward by Konstantin Tsiolkovsky[1] in 1924 and then later expanded on by Shad and Moriarty[2] who first proposed the concept of launching objects specifically with beamed microwave energy from a ground-based source. Since the work of Shad and Moriarty, a great deal of research has been done leading to a wide variety of beamed microwave propulsion concepts as well as significant advances in microwave generation.

Launch concepts based on beamed energy propulsion can fall into one of three categories: 1) direct energy coupling to the propellant, 2) energy addition to a heat exchanger, or 3) energy coupling via plasma formation. This analysis will look at directly coupling microwave energy to the effluents of a solid rocket motor in the diverging section of the nozzle. Through direct energy coupling, this concept involves augmenting the thrust of an existing rocket by first heating liquid alumina particles produced by the thruster, then transferring that energy to the expanding gas via gas-particle collisions. Simply augmenting the thrust of an existing rocket has several distinct advantages. First, since the microwave energy radiates from a remote, ground-based source, the mass increase on the vehicle itself is minimal. Second, only the diverging section of the nozzle would need altering to handle higher temperature operation since the power addition only occurs in this section. Finally, the enhanced performance, provided by this beamed propulsion concept, can lead to the reduction in the complexity of launch vehicle staging and possibly single stage to orbit operation. Thrust augmentation using beamed energy does have several drawbacks. First, microwave coupling to supersonic, two phase flow needs to be investigated. Next, the redesign of the

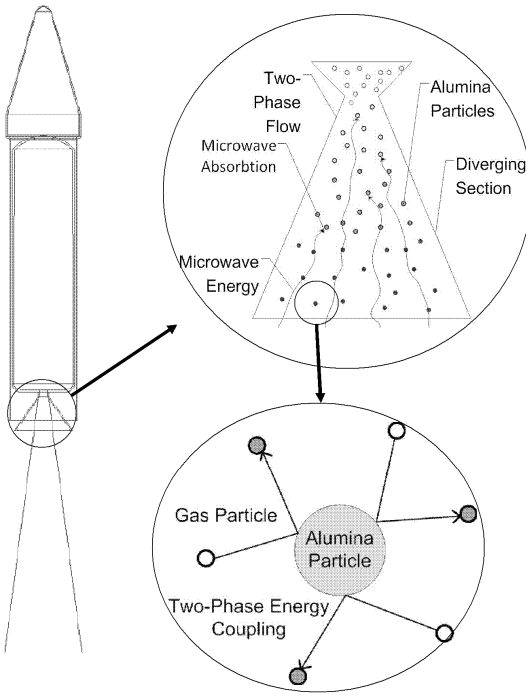

Figure 1. Microwave thrust augmentation through direct coupling to alumina particles.

nozzle is required to handle high temperature loads. Finally, because large power densities are required, the infrastructure cost of such a ground-based facility will be quite high.

The second of the aforementioned categories has been studied primarily by Parkin.[3] Through his research, he has developed a concept for a "Microwave Thermal Thruster" which involved beaming microwave power to a heat exchanger attached to the launch vehicle. The heat exchanger absorbs the energy and transfers it to a hydrogen propellant flowing through an array of small channels. Parkin et al. indicate that a hydrogen propellant is capable of producing 54 kN of thrust with a specific impulse of over 1000 seconds.[4] Parkin and Culick estimate that a one metric ton vehicle can carry 100 kg of payload to an 1100 km circular orbit using 275 MW of beamed energy.[5] This system offers the benefit of higher exhaust velocities over traditional chemical rockets and thus higher specific impulse.

Researchers at the University of Tokyo have investigated a concept utilizing beamed microwave energy to produce plasma near the focal point of the directed beam.[6, 7] The formed plasma then absorbs the remaining microwave pulse to increase the enthalpy of the propellant. The vehicle utilizes repetitive pulses to induce plasma in either the stored propellant or the air to propel the vehicle. Both the systems proposed by the researchers at the University of Tokyo and Parkin et al. use the beamed power as the sole source of propulsive force. The concept in this manuscript (where microwave augmentation merely enhances the vehicle performance) can be viewed as a short term alternative to these aforementioned concepts. This could significantly reduce the risk of attempting to launch an initial beamed microwave vehicle while providing a technology demonstration for the concepts derived by other authors. Other advantages to the proposed concept include no mass increase due to a heat exchanger and no energy losses due to plasma formation.

In this study, the performance of a notional Castor 120™ is studied in both un-augmented and augmented scenarios. Although the Castor 120™ solid rocket motor is by no means optimized for a thrust augmentation application, it provides a baseline design with well quantified performance characteristics. The performance of this case was evaluated using computational methods through the Program for the Optimization of Simulated Trajectories (POST II).[8] The un-augmented mass and performance characteristics of the Castor 120™ are shown in Table 1.[9] In the augmented case, the Castor 120™ is augmented for the first 50 km of its vertical ascent. An altitude of 50 km was chosen based on potential beam propagation issues through the atmosphere beyond this altitude. An augmentation factor of 1.4 was nominally used is this part of the study. This augmentation factor corresponds to the alumina particles in a Castor 120™ nozzle reaching their boiling point at 3200K with microwave energy addition. The critical analysis presented in this manuscript is three-fold. First, an experimental analysis is presented involving the microwave coupling efficiency of aluminum oxide (alumina) particles to a 2.45 GHz microwave power source. The analysis includes an experimental setup as well as preliminary results. Second, an analytical study is presented on the microwave generation aspect of the system. This work involves determining the basic design concept parameters for a nominal remote power source. Finally, a computational study is presented using POST II that evaluates the gains of augmenting the thrust, as well

Table 1. Castor 120 Characteristics.

Characteristic	Value	Characteristic	Value
Burn Time	79 s	Wet Mass	530,767 kg
Average Vacuum Thrust	1,687,655 N	Dry Mass	4071.5 kg
Maximum Vacuum Thrust	1,881,597 N	Propellant Mass	49,005.2 kg
Average Pressure	8.58 MPa	Mass flow rate	620.31 kg/s
Maximum Pressure	9.99 Mpa	Throat diameter	0.365 m
Specific Impulse	280.2 s	Exit diameter	1.52 m
Exit Velocity	2,000 m/s	Expansion Ratio	24

as power requirements to obtain desired thrust augmentation factors.

Microwave Coupling

The process of coupling microwave energy to alumina particles in the solid rocket motors exhaust is paramount to assess the potential of this concept study. The thrust augmentation process can be achieved in one of two ways: 1) heating alumina droplets with microwave energy and transferring that energy to the expanding gas through collisions, or 2) vaporizing the alumina droplets through the microwave energy and adding molecular species to the flow. Because of the relatively high latent heat of vaporization of alumina, vaporization is not expected to contribute to the overall augmentation process. Therefore, thrust augmentation will occur in a two step process. First, the alumina particles will be heated in the nozzle (through microwave addition) from their nominal combustion chamber temperature of approximately 2500 K to their boiling temperature of approximately 3250 K. Constant microwave energy addition will allow the particles to maintain a temperature of 3250 K throughout the nozzle. The particles then are used as a heat exchanger with the surrounding gas. Through gas-particle collisions, the gas enthalpy is increased. As the gas expands through the nozzle, it converts the imparted thermal energy to kinetic energy, thus increasing the thrust. This augmentation process is depicted in Fig. 1. For the purposes of this study, an experiment was conducted to investigate the coupling capability of alumina particles with microwave energy.

Experimental Setup

Results from Weber et al.[10] give an absorption coefficient for molten alumina in the visible wavelength range from 0.385 to 0.780 μm. Thostenson and Chou[11] investigate the effects of radiating ceramic powders in the microwave range. The purpose of this experiment is to generate a coupling efficiency for solid alumina particles at 2.45 GHz. To back out a coupling efficiency of microwave energy to alumina particles a comparison of the power of a 2.45 GHz system was done in relation to a standard plate heater to a steady state temperature. A sample of alumina power with an average particle size of 10 microns was radiated in a 0.23 m^3 Faraday cage with a 2.45 GHz magnetron. The temperature of the particles was read using a Mikron Infrared MI-S12AL pyrometer from outside the Faraday cage. A diagram of the experimental setup is shown in Fig. 2. First, a sample of 0.0775 kg of alumina particles was irradiated with the magnetron until they reached a steady state temperature. Temperature samples were then taken a rate of 1 Hz for the period of one hour. Power for the microwave system was measured using an Agilent E4419B EPM Series power meter. The alumina particles were then heated using an Omega QC-061040-T quartz faced panel heater to the same steady state temperature. The heater voltage was varied using a variable transformer and the power from the heater was extracted by measuring the current and voltage with an amp meter and digital multimeter respectively. The temperature was monitored using the same pyrometer setup as the microwave test at the same emissivity. To obtain the coupling coefficient for the alumina particles, the ratio of power from the heater to the power from the microwave system (at the same steady state temperature) was calculated.

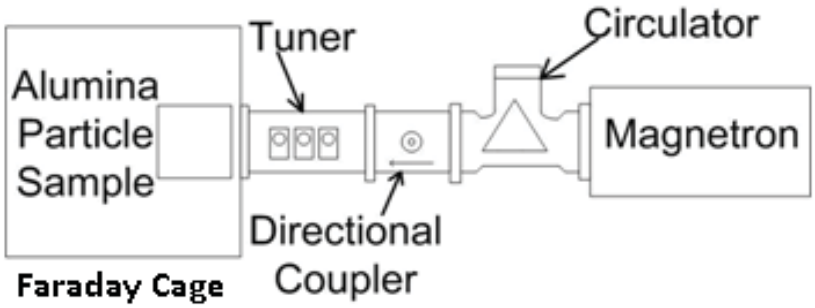

Figure 2. Experimental Setup.

Results

During the microwave test, the alumina powder reached a steady state temperature of approximately 543°C after a period of 42 minutes as shown in Fig. 3. The downstream microwave power level reaching the alumna powder during this test remained relatively constant at 1.811 kW. Within 10 seconds of full microwave power, the particles in the powder began to glow orange, indicating rapid energy absorption. The sample was then cooled and reheated using the plate heater to the same steady state temperature. The voltage input and current of the heater was recorded as 159.0 V and a 6.5 A yielding a power of 1.033 kW. Therefore, the efficiency of microwave absorption by alumina particle was found to be 57.1%.

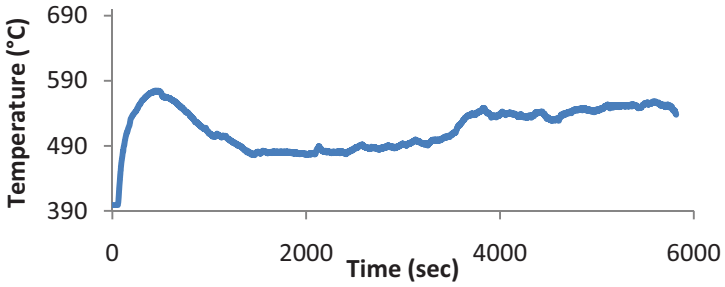

Figure 3. Pyrometer Temperature data for microwave irradiation of alumina particles.

In developing the coupling efficiency several assumptions were made. First, the losses due to convection cooling and conduction through the Faraday cage were assumed to be the same for both the microwave and resistive heater configurations, and therefore were neglected in the calculations. Also, the emissivity of the sample was assumed to be constant through the heating process. The instrumentation in this experiment induced a certain amount of error in the power calculations. The microwave power meter has a resolution of 4 W and an accuracy error of 0.01% yielding a percent error of 0.1 %. The digital multimeter and amp meter measurements have errors of 0.7% and 3.8% respectively. The substantial error in the amp meter measurements stems from a low resolution of 0.5 A. Using a sequential propagation uncertainty analysis the total coupling efficiency error due to instrumentation was 2.2%.

Microwave Generation

One of the key components to this thrust augmentation analysis is the ground based microwave generation system. In order to utilize this system as a short term alternative to other proposed beamed energy methods, a requirement was that the technology used for this concept design be readily available. This analytical study outlines the key components in developing a beamed power generation system.

Antenna Structure

The proposed antenna system structure and its components are outlined by J. Benford R. Dickinson.[12] The system consists of an array of parabolic antenna apertures in phase lock to maximize the transmitted wave output. This system closely resembles a passive phased array system which features a phase shifter at each radiating element and uses high power microwave tubes (magnetrons, travelling wave tubes, klystrons, gyrotrons, etc.) as the wave source. The passive phased array design was chosen over a typical active phased array system which utilizes transmit/receive (T/R) modules for phase control and final amplification. Passive phased array systems tend to be simpler, more reliable, and more efficient. In Benford and Dickinson's proposed system, each array module will consist "of thermally controlled elevation over azimuth (AZ-EL), beam waveguide (BWG) parabolic antenna about 9 m in diameter...The gyrotron transmitter and the low noise amplifier (LNA) receiver are housed in the antenna pedestal and are duplexed to the BWG feed system via a flip-mirror arrangement." The fundamental array module components for the system proposed in this paper will follow Benford and Dickinson's model. A diameter of 9 m was set in Ref. 12 and is considered optimal when dealing with the ease of mechanical antenna tracking and steering as well as element cost.

Microwave Source

One important aspect of developing a microwave power beaming system was considering the microwave energy source. In recent years there have been considerable advances in microwave source technology suitable for power beaming. Of these, most notably, is the free electron laser (FEL) and the gyrotron family. Both are capable of producing high frequency waves (in the lower terahertz regime) at high average power. Figure 4 shows the evolution of power generating capability for available microwave sources.[13]

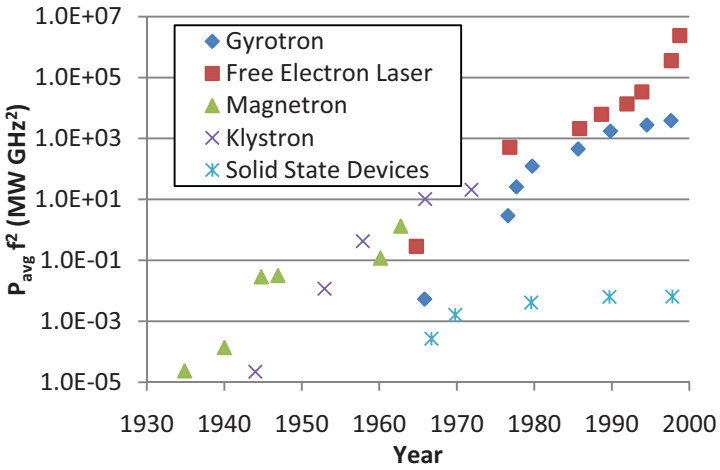

Figure 4. Recent advances in microwave source technology (after Ref. 13).

Both FELs and gyrotrons work on the principle of converting spontaneous electromagnetic radiation into coherent radiation via the beam-wave interaction.[13] Currently, gyrotrons are being used to produce waves in the 100 to 280 GHz frequency range at the MJ level. Commercially available gyrotrons are capable of producing 140 GHz at 1 MW average power in a continuous wave (CW) operation. It was preferred for this concept design that the gyrotrons be operated as amplifiers rather than oscillators due to the ease of beam steering through the phase shifters. Steering in this case is done simply by phase shifting the module drive signal. However, it is plausible to achieve phase control with a system featuring oscillators; although it must also include "means such as a magnetic field strength trim to set the rest frequency of the oscillator or to periodically measure static phase".[12]

Frequency

Another important aspect of the system to consider was the transmitted frequency. Atmospheric breakdown and attenuation play key roles in selecting a frequency. The breakdown fluence (in W/m^2) is given by Eq. (1):

$$\phi = 2.39p^2 + 2.39p^2 \frac{\omega^2}{\upsilon^2} \tag{1}$$

The molecular collision frequency, ν, for air is 5.3 x 10^9p(s^{-1}). Atmospheric gasses beak down (form plasma) easier at low pressure and low frequencies; moreover, losses due to breakdown would be detrimental to the system. The necessary high power at high altitudes for this concept design requires a system that operates with a higher frequency (preferably in the millimeter wave length range). Figure 5 was generated using empirical data from Crane and Blood[14] and shows the atmospheric attenuation for this frequency range. Windows at approximately 35, 94, 140, and 245 GHz exist where atmospheric attenuation is minimal.

A slew of factors were considered when determining a frequency. For example, a higher frequency reduces the necessary size of the antenna for a given antenna gain as shown in Eq. (2).

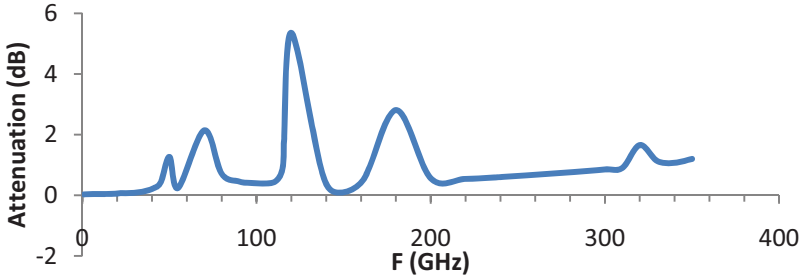

Figure 5. Atmospheric attenuation for the low terahertz frequency range.

$$G_{dbi} = 20\log\left(\eta_r \frac{\pi D}{\lambda}\right) \quad (2)$$

With this reduction in size, choosing a higher frequency (say 140 or 245 GHz) was beneficial. Another critical factor is free space loss. Higher frequencies yield higher free space losses as indicated by Eq. (3).

$$L_{fs} = 20\ \log_{10}\left(\frac{4\pi R}{\lambda}\right) \quad (3)$$

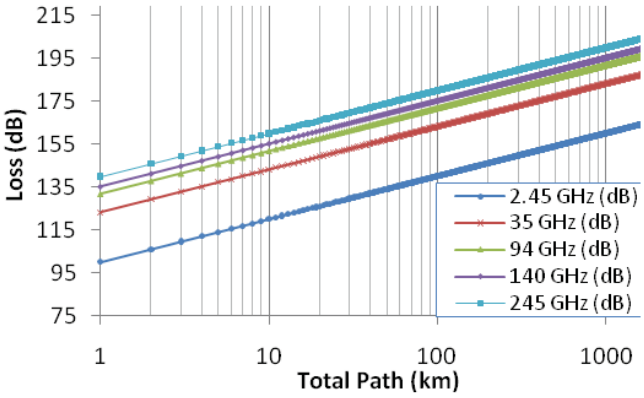

Figure 6. Free space loss as a function of frequency.

Figure 6 shows the effects of frequency on free space loss. Taking these factors into account, the optimum frequency for the proposed system is set at 140 GHz. This is at the lower bound of the terahertz frequency range which extends from 0.1 THz to 10 THz.

Power Budget

To determine the required number and size of the antenna elements, the spot area (the area on the nozzle that contains at least half the power density) must be defined. The effective diameter for the antenna array required for a give spot area (at a given altitude) is determined by using a modified diffraction formula depicted in Eq. (4).[3]

$$D = \frac{2.44\lambda/\theta_{beam}}{\sqrt{\cos(\theta_z)}} \quad (4)$$

The beamwidth can be determined from the spot area of the beam assuming the antenna array radiates in a perfect cone. A spot diameter of 1.5 m was chosen which corresponds to the diameter of the Castor 120™ nozzle. As stated above, the range is limited to 50 km due to power attenuation beyond that distance. Assuming a zenith transmission, the corresponding effective diameter for the array was 207 m. A power budget analysis can then determine the required transmitted power and number of elements. Traditional methods for power budgeting include performing a link budget analysis through the system's gains, losses, and power output, expressed in logarithmic form by Eq. (5).

$$P_r = P_t + G_t + G_r - L_{fs} - L_{atm} - L_{other} \quad (5)$$

However, using the link budget analysis for determining power is not appropriate for the proposed system. The link budget assumptions, and therefore the governing equations, are only valid for far field approximations defined in the region approximated by Eq. (6).

$$R_{ff} = \frac{2D^2}{\lambda} \quad (6)$$

At an effective diameter of 207 m and a frequency of 140 GHz, the antenna array has a far field region well beyond operation range. Therefore, for operation in the near field, an alternative power budget method must be used. According to W. C. Brown[15], free space power transmission can be represented through a series of efficiencies to determine the necessary power requirements. The overall efficiency of the system is divided into several sub-efficiencies and takes the form of Eq. (7).

$$\eta_t = \eta_1\eta_2\eta_3 \ldots \eta_n \quad (7)$$

Parkin[3] utilized this power budget method in his thesis on microwave thermal thrusters. The most pertinent sub-efficiency is the general transmission efficiency which is a function of the system's transmission range, frequency, and antenna aperture size (similar to a link budget analysis). A path loss parameter, τ, is first defined in Eq. (8).[15]

$$\tau = \frac{\sqrt{A_r A_t}}{\lambda D} \qquad (8)$$

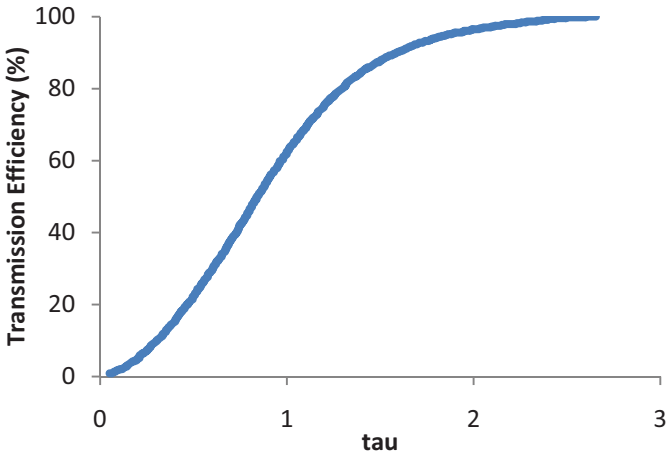

Figure 7. Transmission efficiency as a function of parameter, τ (after Ref. 15).

The relationship between path loss efficiency and τ is shown in Fig. 7[15] and was proven mathematically by Goubau and Scherwing.[16] The design parameters for this power budget method are as follows: the transmitted frequency is 140 GHz, the range is 50 km, the transmitter antenna has an effective diameter of 207 m, the received power at the nozzle is 1 GW, and the spot diameter at the nozzle is 1.5 m. This yields a τ value of 2.28. From Fig. 7, the path loss efficiency was conservatively estimated at 90%. The remaining sub-efficiencies and their values were formulated from a combination of both papers by Parkin[3] and Brown[15] and are shown in table 2. Using this power budget method yields a required transmitted power of 3.125 GW through 529 antenna elements at 9 m in diameter.

Table 2. Sub-efficiency values for power budget

Efficiency	Value
Path loss efficiency	90%
Generator Electronic	92%
Generator Circuit Efficiency	61%
Atmospheric Transmission Efficiency	89%
Illumination Efficiency	88%

The designed system will produce 1 GW of peak microwave power with a spot diameter of 1.5 m at a range of 50 km. In the case that the launch vehicle requires more than 1 GW of microwave power augmentation, this array system can act as a sub-array to a larger system. For instance, if 5 GW of total power is needed at the nozzle, it is reasonable to assume that five of the proposed arrays can be combined to produce the necessary power provided that the antenna as a whole is in phase.

Performance and Power

Power requirements needed at the launch vehicle as well as the potential gains achieved by the augmentation of the thrust were explored using computational methods. Velocity data and power data that are presented were acquired with the use of Program to Optimize Simulated Trajectories (POST II).[8] Simulations were performed for an ATK Castor 120™ solid rocket motor without payload.[9] The trajectory of the launch vehicle was done for a stationary (non-rotating) oblate earth using the 1962 US standard atmosphere model with no atmospheric winds. The simulated trajectory guidance was done to an altitude of 50 km at an azimuth of 89 degrees with no pitch, roll, or yaw for the launch vehicle. Thrust data was obtained through the evaluation and interpolation of known vacuum thrust models for the Castor 120™.[9]

The total power input for the system was calculated using thrust data and applying the equation for total jet power.[9,18]

$$P_{in\ jet} = \frac{1}{2}\dot{m}V_e^2 \quad (9)$$

The power output of the system was calculated from the simulations and an evaluation of the total kinetic and potential energy of the system was performed at each interval of the thrust augmentation multiplication factor.[8] The power output was then determined from the energy and burn time to 50 km.

$$P_{out} = \frac{E_{t,50km}}{t_{50km}} \quad (10)$$

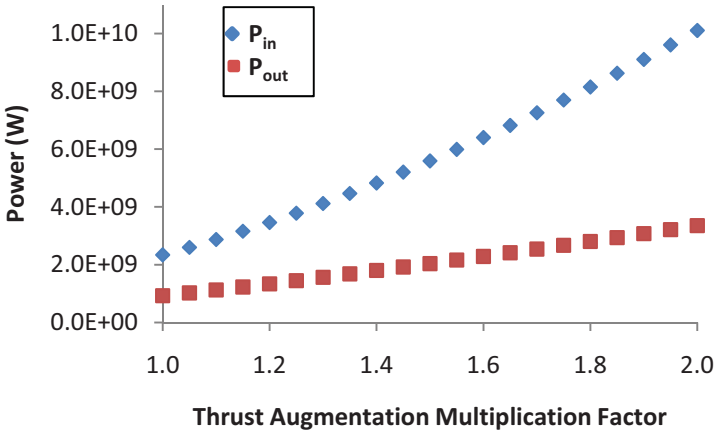

Figure 8. The derived total power for the launch vehicle with respect to percent increase of thrust augmentation.

The upper set of data points in Fig. 8 represent the total jet power input into the system from the rocket and the microwave system. The lower set of data points in the figure represent the total kinetic and potential power output by the system. The trend in this figure between the input and output power illustrates the increasing difference in power in versus power out with the augmentation of the thrust.

The change in the power input (power added by microwave system) was calculated by evaluating the difference in jet power between the standard jet power of a Castor 120™ and the augmented power derived from the simulations. The change in the power output was then calculated in the same manner. For the vehicle thrust to increase by a factor of 1.4 it is noted that the power input into the system must be doubled. This relationship continues to increase with respect to the increase in thrust augmentation. For an increase in thrust of 40%, the microwave system would need to produce an average of 4.39 GW at the launch vehicle nozzle assuming a 57.1 % coupling efficiency.

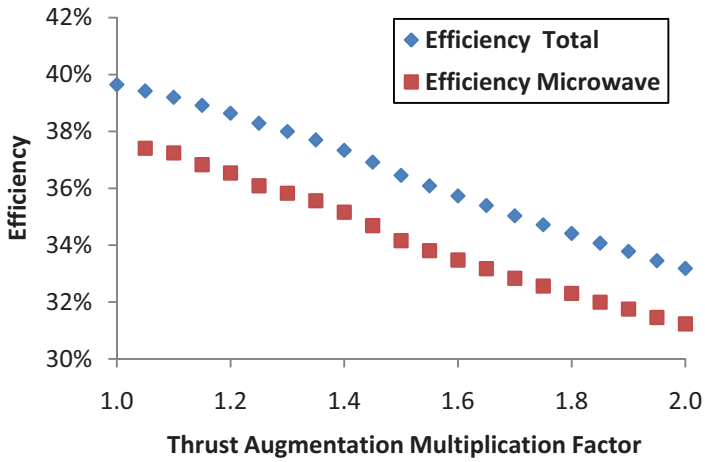

Figure 9. Efficiency model of the launch vehicle in relation to the percent increase of thrust augmentation.

The efficiency of the system was determined for two separate aspects in Fig. 9. First, the total efficiency was calculated by evaluating the total power output to the total input jet power of the launch vehicle with respect to the thrust multiplication factor. Second, the efficiency of the microwave system was evaluated by comparing the change in the power output versus the difference in jet power input into by the microwave system.

$$\eta_{\mu wave} = \frac{\Delta P_{out}}{\Delta P_{in\ jet}} \quad (11)$$

The trend in Fig. 9 illustrates that as the thrust augmentation is increased over 50 kilometers the efficiency of both the total launch vehicle and the microwave system decrease. This decrease in efficiency is due primarily to the higher velocities reached at lower altitudes. This increased velocity yields higher losses in the lower atmosphere due primarily to drag. However this decrease in efficiency is traded for a higher change in velocity at burn out and a higher specific impulse.
The greatest gain seen with the augmentation of the thrust is the increase in velocity (ΔV). The upper set of data points in Fig. 10a represent the change in velocity from the Earth's surface to a height of 50 km. The lower set of data points correspond to the change in ΔV at 50 km compared to the un-augmented ΔV. The ΔV of launch vehicle with respect to thrust augmentation at 50 km shows a steady increase with respect to the thrust augmentation multiplication factor. The un-augmented velocity of a Castor 120™ with the given trajectory is approximately 2.322 km/s at 50 km. With a thrust multiplication factor of 1.4 the velocity of the model at 50 km increased to 2.587 km/s, for a total change in velocity of 264 m/s and an increase in specific impulse from 280 seconds to 402 seconds. The velocity of the same case at burnout changed by approximately 1 km/s with an increase in height of 50 km at burnout.

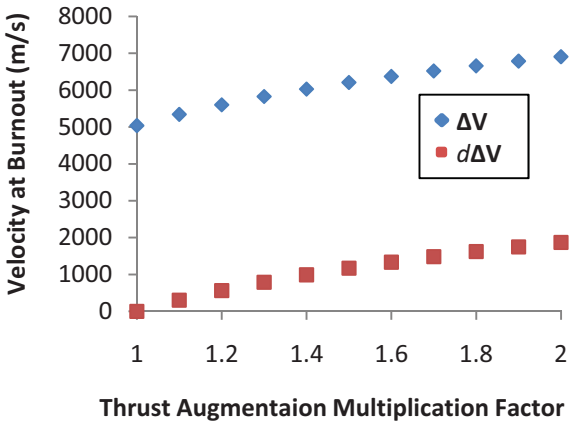

Figure 10a. Change in velocity seen at burn out in relation to an absolute and relative change in velocity.

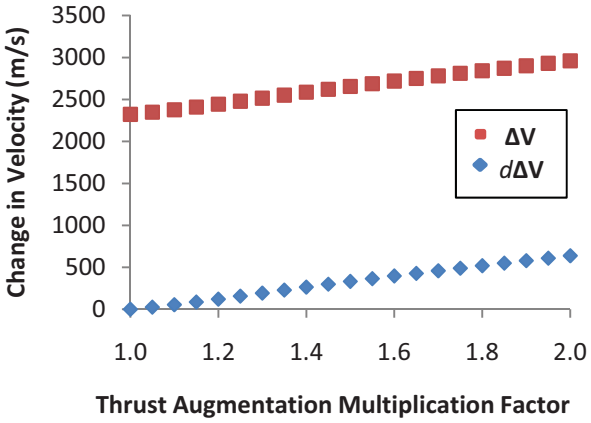

Figure 10b. Change in velocity seen at 50 km in relation to an absolute change and a relative change velocity.

In Fig. 10b the change in ΔV at burn can be seen as high a 1.86 km/s (lower set of data points). The upper set of data points in the figure represents the ΔV of the launch vehicle with respect to the thrust augmentation multiplication factor. The given trajectory causes the vehicle to essentially ascend straight up for 50 km and then begin making its gravity turn into orbit. This trajectory causes an extreme amount of additional forces on the launch vehicle during the turn. Alternate trajectory paths may need to be explored in order to minimize these effects. With the increase in velocity at burnout, created by augmentation of the thrust of the vehicle with microwaves, it is possible for a vehicle, which would not otherwise be able to reach the appropriate orbital velocity, to achieve an orbit.

Discussion

Results from the microwave coupling experiment indicate that alumina particles absorb microwave energy with an efficiency of 57.1%. For the nominal microwave generation system proposed in this analysis where 1 GW of power is produced at the vehicle nozzle, only 0.57 GW actually gets absorbed for thrust augmentation. The increase in thrust corresponding to 0.57 GW is a mere factor of 1.1 thus yielding an increase in ΔV of 305 m/s at burnout. Figure 11 depicts the nominal thrust augmentation system in this study.

Conclusion

The advantages of beamed energy propulsion over current rocket systems are highlighted by the ability to overcome the specific impulse limitations presented in traditional chemical rockets. The works from Parkin et al. and the researchers at the University of Tokyo outline pure beamed energy propulsions systems for future implementation. The purpose of this critical analysis was to explore a shorter term alternative beamed energy system in which rocket thrust is merely augmented. Microwave coupling to alumina particles formed the basis for this concept. The analysis first explored the coupling efficiency of alumina particles to microwave energy. Preliminary results indicate that a coupling efficiency on the order of 57% is possible for solid alumina particles radiated with microwave energy. Further investigation must include electromagnet radiation effects on molten alumina droplets at various frequencies as well as an analysis on the gas particle collisions needed to transfer the added energy. This study also explores a possible concept design for the ground based microwave source that utilizes readily available technology. To produce a nominal 1 GW of microwave power at 50 km, the system must produce approximately 3.13 GW of power through 529 antenna elements. Although the technology for this system is readily available, the cost to implement this system would be prohibitive. Further advances in high power microwave sources might alleviate the initial infrastructure cost. Power levels well beyond 1 GW might be necessary at the nozzle in order for a vehicle to reach orbital velocity. With the power demands of larger solid rocket motors, it is noted that the launch vehicle must be optimized for lower powers to be advantageous. Additional limitations in this process are seen with the maximum temperature increase in the nozzle set at the boiling point of the alumina droplets. With the increased velocity and drag at low altitude it may also be necessary to increase the structural integrity of the launch vehicle to handle the amplified aerodynamic and gravitational forces.

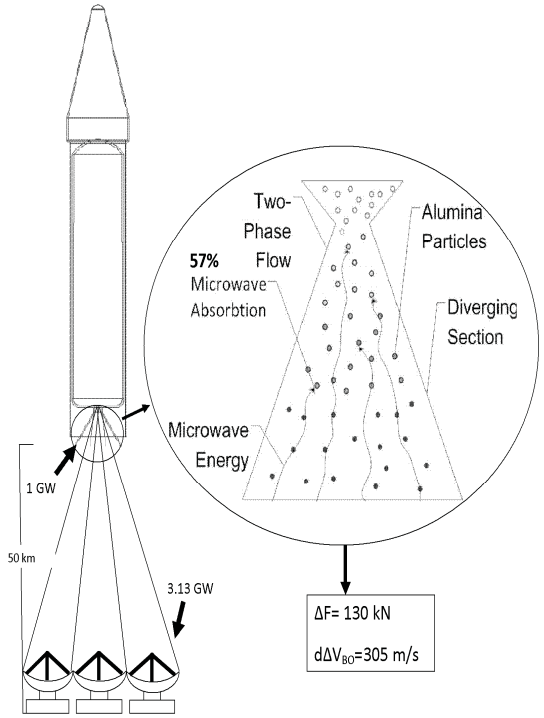

Figure 11. Microwave thrust augmentation model.

Acknowledgements

This work was funded by the Advanced Concepts Group of the Air Force Research Laboratory, Propulsion Directorate, Edwards AFB, California. The authors are grateful to Dr. Marcus Young (AFRL/RZSA) and Dr. Andrew Ketsdever for their support of this work. The authors are also grateful to the Mechanical and Aerospace Engineering Department for their contributions.

References

[1]Tsiolkovsky(1924). *Spaceship,* 1924, in Izbrannye Trudy, Compiled by Vorob'ev, B.N., Sokol'skii V.N., General Editor Acad. Blagonravov, Izdatel'stvo Akademii Nauk SSSR, Moscow, Russia, 1962, 222 (in Russian). Edited Machine Translation prepared by Translation Division, Foreign Technology Division, WPAFB, Ohio, on May 5th, 1966, 307.

[2]Shad, J. L., and Moriarty, J. J., "Microwave Rocket Concept," in XVI International Astronautical Congress, Athens, 1965.

[3]Parkin, K. G., "The Microwave Thermal Thruster and its Application to the Launch Problem," Ph.D. Dissertation, California Institute of Technology, Pasadena, CA, 2006.

[4]Parkin, K. G., DiDomenico, L. D., and Culick, F., "The Microwave Thermal Thruster Concept," *Proceedings of the Second International Symposium: Beamed Energy Propulsion*, ed. K. Komurasaki, AIP Conference Proceedings 702, Melville, NY, 2004, pp. 418-429.
[5]Parkin, K. G., and Culick, F., "Feasibility and Performance of the Microwave Thermal Rocket Launcher," *Proceedings of the Second International Symposium: Beamed Energy Propulsion*, ed. K. Komurasaki, AIP Conference Proceedings 702, Melville, NY, 2004, pp. 407-417.
[6]Oda, Y., Komurasaki, K., Takahashi, K., Kasugai, A., and Sakamoto, K., "Plasma Generation Using High-Power Millimeter-Wave Beam and Its Application for Thrust Generation," *J. Appl. Phys.*, Vol. 100, 113307, 2006.
[7]Nakagawa, T., Yorichika, M., Komurasaki, K., Takahashi, K., Sakamoto, K., and Tsuyoski, I., "Propulsive Impulse Measurement of a Microwave-Boosted Vehicle in the Atmosphere," *J. Spacecraft and Rockets*, Vol. 41, No. 1, pp. 151-153, 2004.
[8]*Program to Optimize Simulated Trajectories (POST II)*, Volume I & II version 1.1.6.G, January 2004.
[9]Hilden, J., and Poirier, B., "Castor 120™ Motor:Development and Qualification Testing Results," *AIAA Paper 93-4277, AIAA Space Programs and Technologies Conference and Exhibits*, Huntsville, AL, September 1993.
[10]Weber, J. K., Krishnan, S., Anderson, C., and Nordine, P., "Spectral Absorption Coefficient of Molten Aluminum Oxide from 0.385 to 0.780 μm," *Journal of American Ceramics Society*, Vol. 78, No. 3, March 1995, pp. 583-587.
[11]Thostenson, E. T., and Chow, T. W., "Microwave Processing: Fundamentals and Applications," *Composites: Part A*, Elsevier Science Ltd., February 1999, pp. 1055-1071.
[12]Benford, J., and Dickinson, R., "Space Propulsion and Power Beaming Using Millimeter Systems," *Intense Microwave Pulses III-SPIE*. Vol. 2557.
[13]Baker, R. J., Booske, J. H., Luhmann, N. C., Jr., and Nusinovich, G. S., *Modern Microwave and Millimeter-Wave Power Electronics*, IEEE Press, Piscataway, NJ, 2005.
[14]Crane, R. K., and Blood, D. W., *Handbook for the Estimation of Microwave Propagation Effects-Link Calculation for Earth-space Paths*, Environmental Research and Technology Inc., Greenbelt, MD, 1979.
[15]Brown, W. C., "The Technology and Application of Free-Space Power Transmission by Microwave Beam," *Proceedings of the IEEE*. 1974, pp. 11-25.
[16] Goubau, G., and Schwering, F., "On the guided propagation of electromagnetic wave beams," *IRE Trans. Antennas Propagat*, Vols. AP-9, 1961.
[17]Kare, J., and Parkin, K., "A Comparison of Laser and Microwave Approaches to CW Beamed Energy Launch," *Proceedings of the Fourth International Symposium: Beamed Energy Propulsion*, ed. K. Komurasaki, T. Yabe, S. Uchida, and A. Sasoh, AIP Conference Proceedings 830, Melville, NY, 2004, pp. 388-399.
[18]Haslett, C., *Essentials of Radio Wave Propagation*, Cambridge University Press, New York, 2008, Chaps 1,2.
[19] Balanis, C. A., *Antenna Theory: Analysis and Design*, Wiley-Interscience, New York, 1997, Chaps 1-4.
[20]Peterson, Philip G., and Hill, Carl R., *Mechanics and Thermodynamics of Propulsion*, Addison-Wesley Publishing Company, Inc., 1992, pp. 656-659.
[21]EMS Technologies Inc., "Passive Phased Arrays for Radar Antennas," Atlanta, GA, 2005.